Experimental and modeling study of *n*-pentane low temperature oxidation. Detection of hydroperoxides, ketohydroperoxides and highly oxygenated molecules using high resolution mass spectrometry

Nesrine Belhadj[1,2,*], Maxence Lailliau[1] , Roland Benoit[1], Philippe Dagaut[1]

[1] CNRS–INSIS, ICARE, Orléans, France

[2] Université d'Orléans, Orléans, France

ACS Spring Meeting, March 20-24, 2022, San Diego, USA

1- Introduction
2- Experimental
3- Results
4- Conclusion and perspectives

1- Introduction

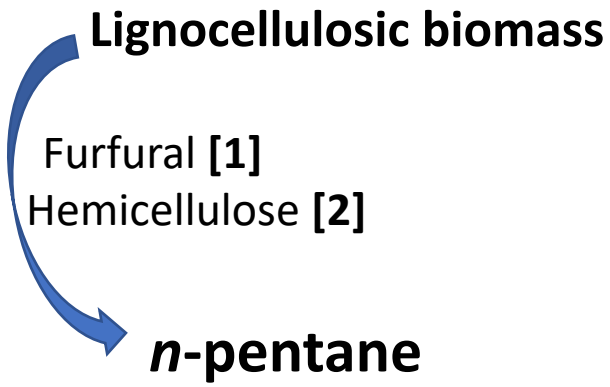

[1] Z. Xinghua; W. Tiejun; M. Longlong; W. Chuangzhi, Aqueous-phase catalytic process for production of pentane from furfural over nickel-based catalysts, Fuel 89 (10) (2010) 2697-2702.
[2] S. Liu; Y. Okuyama; M. Tamura; Y. Nakagawa; A. Imai; K. Tomishige, Selective transformation of hemicellulose (xylan) into n-pentane, pentanols or xylitol over a rhenium-modified iridium catalyst combined with acids, Green Chemistry 18 (1) (2016) 165-175.

1- Introduction

Lignocellulosic biomass

Furfural **[1]**
Hemicellulose **[2]**

***n*-pentane** → biofuel additive **[3,4]** → Enhance performance of diesel and gasoline engines; Environmental benefits (reduction of NO_x, HC, and CO emissions)

[1] Z. Xinghua; W. Tiejun; M. Longlong; W. Chuangzhi, Aqueous-phase catalytic process for production of pentane from furfural over nickel-based catalysts, Fuel 89 (10) (2010) 2697-2702.
[2] S. Liu; Y. Okuyama; M. Tamura; Y. Nakagawa; A. Imai; K. Tomishige, Selective transformation of hemicellulose (xylan) into n-pentane, pentanols or xylitol over a rhenium-modified iridium catalyst combined with acids, Green Chemistry 18 (1) (2016) 165-175.
[3] M. Elkelawy; H. Alm-Eldin Bastawissi; E. A. El Shenawy; M. Taha; H. Panchal; K. K. Sadasivuni, Study of performance, combustion, and emissions parameters of DI-diesel engine fueled with algae biodiesel/diesel/n-pentane blends, Energy Conversion and Management: X 10 (2021) 100058.
[4] H. Jin; J. Pieper; C. Hemken; E. Bräuer; L. Ruwe; K. Kohse-Höinghaus, Chemical interaction of dual-fuel mixtures in low-temperature oxidation, comparing n-pentane/dimethyl ether and n-pentane/ethanol, Combust. Flame 193 (2018) 36-53.

Since several decades, kinetic and experimental oxidation of *n*-alkanes in combustion systems (flow reactors, jet stirred-reactors, motored engine, and rapid compression machines) received much attention **[5-20]**

[5] Chen, B.; Ilies, D. B.; Hansen, N.; Pitsch, H.; Sarathy, S. M. Simultaneous Production of Ketohydroperoxides from Low Temperature Oxidation of a Gasoline Primary Reference Fuel Mixture. *Fuel* **2021**, *288*, 119737.
[6] Herbinet, O.; Husson, B.; Gall, H. L.; Battin-Leclerc, F. An Experimental and Modeling Study of the Oxidation of N-Heptane, Ethylbenzene, and n-Butylbenzene in a Jet-Stirred Reactor at Pressures up to 10 Bar. *International Journal of Chemical Kinetics* **2020**, *52* (12), 1006–1021.
[7] Guo, J.; Peng, W.; Zhang, S.; Lei, J.; Jing, J.; Xiao, R.; Tang, S. Comprehensive Comparison of the Combustion Behavior for Low-Temperature Combustion of n-Nonane. *ACS Omega* **2020**, *5* (10), 4924–4936.
[8] Wang, Z.; Chen, B.; Moshammer, K.; Popolan-Vaida, D. M.; Sioud, S.; Shankar, V. S. B.; Vuilleumier, D.; Tao, T.; Ruwe, L.; Bräuer, E.; Hansen, N.; Dagaut, P.; Kohse-Höinghaus, K.; Raji, M. A.; Sarathy, S. M. N-Heptane Cool Flame Chemistry: Unraveling Intermediate Species Measured in a Stirred Reactor and Motored Engine. *Combustion and Flame* **2018**, *187*, 199–216.
[9] Mével, R.; Chatelain, K.; Boettcher, P. A.; Dayma, G.; Shepherd, J. E. Low Temperature Oxidation of N-Hexane in a Flow Reactor. *Fuel* **2014**, *126*, 282–293.
[10] Karwat, D. M. A.; Wagnon, S. W.; Wooldridge, M. S.; Westbrook, C. K. Low-Temperature Speciation and Chemical Kinetic Studies of n-Heptane. *Combustion and Flame* **2013**, *160* (12), 2693–2706.
[11] Herbinet, O.; Husson, B.; Serinyel, Z.; Cord, M.; Warth, V.; Fournet, R.; Glaude, P.-A.; Sirjean, B.; Battin-Leclerc, F.; Wang, Z.; Xie, M.; Cheng, Z.; Qi, F. Experimental and Modeling Investigation of the Low-Temperature Oxidation of n-Heptane. *Combustion and Flame* **2012**, *159* (12), 3455–3471.
[12] Jia, M.; Xie, M. A Chemical Kinetics Model of Iso-Octane Oxidation for HCCI Engines. *Fuel* **2006**, *85* (17), 2593–2604.
[13] Curran, H. J.; Gaffuri, P.; Pitz, W. J.; Westbrook, C. K. A Comprehensive Modeling Study of Iso-Octane Oxidation. *Combustion and Flame* **2002**, *129* (3), 253–280.
[14] Minetti, R.; Carlier, M.; Ribaucour, M.; Therssen, E.; Sochet, L. R. A Rapid Compression Machine Investigation of Oxidation and Auto-Ignition of n-Heptane: Measurements and Modeling. *Combustion and Flame* **1995**, *102* (3), 298–309.
[15] Sahetchian, K.; Champoussin, J.; Brun, M.; Levy, N.; Blin-Simiand, N.; Aligrot, C.; Jorand, F.; Socoliuc, M.; Heiss, A.; Guerassi, N. Experimental Study and Modeling of Dodecane Ignition in a Diesel Engine. **1995**.
[16] Lindstedt, R. P.; Maurice, L. Q. Detailed Kinetic Modelling of N-Heptane Combustion. *Combustion Science and Technology* **1995**, *107* (4–6), 317–353.
[17] Dagaut, P.; Reuillon, M.; Cathonnet, M. High Pressure Oxidation of Liquid Fuels from Low to High Temperature. 2. Mixtures of n-Heptane and Iso-Octane. *Combustion Science and Technology* **1994**, *103* (1–6), 315–336.
[18] Chakir, A.; Bellimam, M.; Boettner, J. C.; Cathonnet, M. Kinetic Study of N-Heptane Oxidation. *International Journal of Chemical Kinetics* **1992**, *24* (4), 385–410.
[19] Axelsson, E. I.; Brezinsky, K.; Dryer, F. L.; Pitz, W. J.; Westbrook, C. K. Chemical Kinetic Modeling of the Oxidation of Large Alkane Fuels: N-Octane and Iso-Octane. *Symposium (International) on Combustion* **1988**, *21* (1), 783–793.
[20] Dryer, F. L.; Brezinsky, K. A Flow Reactor Study of the Oxidation of N-Octane and Iso-Octane. *Combustion Science and Technology* **1986**, *45* (3–4), 199–212.

Investigation of the combustion and the cool flame oxidation of *n*-pentane is of interest for researchers **[21-24].**

Different analytical methods have been developed to identify low-temperature oxidation species, such as pentenyl-hydroperoxides (ROOH), and pentenyl-ketohydroperoxides (KHPs) **[25-29].**

[21] Blin-Simiand, N.; Rigny, R.; Viossat, V.; Circan, S.; Sahetchian, K. Autoignition of Hydrocarbon/Air Mixtures in a CFR Engine: Experimental and Modeling Study. *Combustion Science and Technology* **1993**, *88* (5–6), 329–348.
[22] Knox, J. H.; Kinnear, C. G. The Mechanism of Combustion of Pentane in the Gas Phase between 250° and 400°C. *Symposium (International) on Combustion* **1971**, *13* (1), 217–227.
[23] Hughes, R.; Simmons, R. F. Cool Flame Phenomena in the Oxidation of N-Pentane. *Combustion and Flame* **1970**, *14* (1), 103–111.
[24] Hughes, R.; Simmons, R. F. The Low-Temperature Combustion of n-Pentane. *Symposium (International) on Combustion* **1969**, *12* (1), 449–461.
[25] J. Bourgalais; Z. Gouid; O. Herbinet; G. A. Garcia; P. Arnoux; Z. D. Wang; L. S. Tran; G. Vanhove; M. Hochlaf; L. Nahon; F. Battin-Leclerc, Isomer-sensitive characterization of low temperature oxidation reaction products by coupling a jet-stirred reactor to an electron/ion coincidence spectrometer: case of n-pentane, Phys. Chem. Chem. Phys. 22 (3) (2020) 1222-1241.
[26] Jin, H.; Pieper, J.; Hemken, C.; Bräuer, E.; Ruwe, L.; Kohse-Höinghaus, K. Chemical Interaction of Dual-Fuel Mixtures in Low-Temperature Oxidation, Comparing n-Pentane/Dimethyl Ether and n-Pentane/Ethanol. *Combustion and Flame* **2018**, *193*, 36–53
[27] A. Rodriguez; O. Herbinet; Z. Wang; F. Qi; C. Fittschen; P. R. Westmoreland; F. Battin-Leclerc, Measuring hydroperoxide chain-branching agents during n-pentane low-temperature oxidation, Proc. Combust. Inst. 36 (1) (2017) 333-342.
[28] J. Bugler; A. Rodriguez; O. Herbinet; F. Battin-Leclerc; C. Togbe; G. Dayma; P. Dagaut; H. J. Curran, An experimental and modelling study of n-pentane oxidation in two jet-stirred reactors: The importance of pressure-dependent kinetics and new reaction pathways, Proc. Combust. Inst. 36 (1) (2017) 441-448.
[29] J. Bugler; K. P. Somers; E. J. Silke; H. J. Curran, Revisiting the Kinetics and Thermodynamics of the Low-Temperature Oxidation Pathways of Alkanes: A Case Study of the Three Pentane Isomers, J. Phys. Chem. A 119 (28) (2015) 7510-7527.

- In this study, the oxidation of n-pentane was performed in a **JSR**. Low temperature oxidation products were characterized.

- **Hydroperoxides**, **ketohydroperoxides** (**KHPs**), and **highly oxygenated molecules** (**HOMs**) resulting from multiple O_2 addition of fuel's radicals were tracked using ultra-high pressure liquid chromatography (**UHPLC**) coupled to atmospheric pressure chemical ionization (**APCI**) and high-resolution mass spectrometry (**HRMS-Orbitrap Q-Exactive**).

- HRMS experimental results were compared to modeling datausing the model of Wang and Sarathy (**WS model**) **[30].**

[30] Z. D. Wang; S. M. Sarathy, Third O-2 addition reactions promote the low-temperature auto-ignition of n-alkanes, Combust. Flame 165 (2016) 364-372

2- Experimental

a. Jet stirred reactor

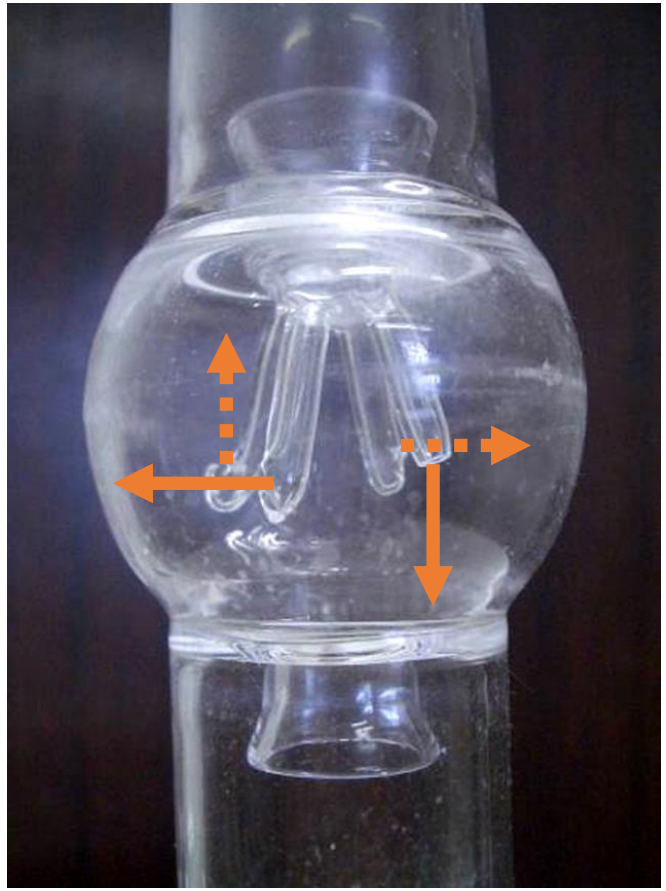

● A fused silica jet-stirred reactor (**JSR**) (c.a. 42 cm^3): 4 injectors (nozzles of 1 mm i.d.), located inside a regulated electrical oven of 1.5kW.

● Flow rates of O_2 (99.995% pure) and N_2 regulated by thermal mass-flow controllers, and fuel by HPLC pump (Shimadzu® LC10 VP).

● *n*-pentane (>99% pure from Sigma-Aldrich®) and O_2 are diluted by N_2 , and injected separately, to avoid oxidation before reaching the injectors .

● Thermal homogeneity is checked using Pt/Pt-Rh10%, 0.1mm diam.

● Oxidation gases are **bubbled in cooled acetonitrile** (0°C, 25 ml, 75 min) after **sonic probe sampling**. Samples are stored in a freezer at -15 °C.

2- Experimental

a. Jet stirred reactor

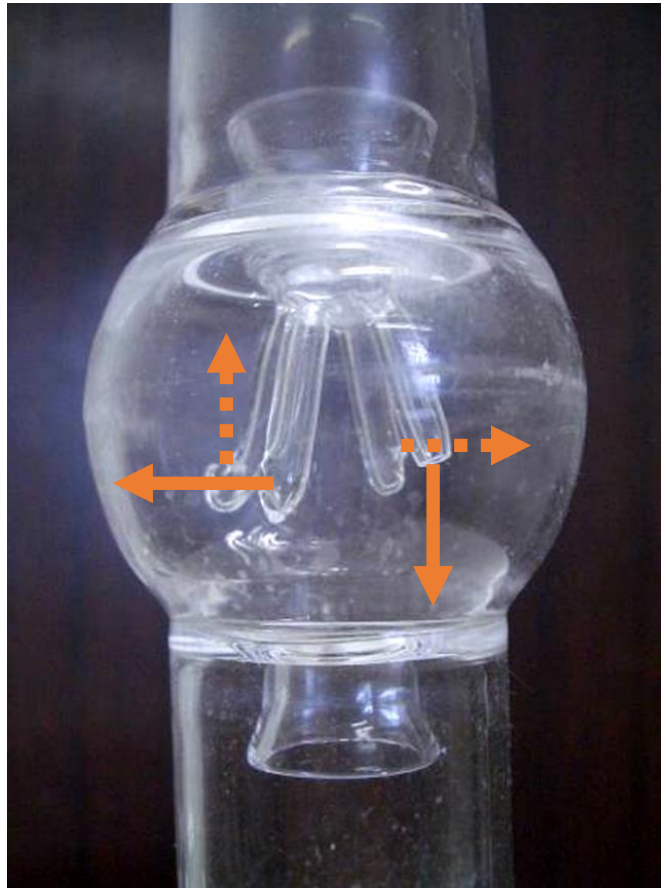

● A fused silica jet-stirred reactor (**JSR**) (c.a. 42 cm^3): 4 injectors (nozzles of 1 mm i.d.), located inside a regulated electrical oven of 1.5kW.

● Flow rates of O_2 (99.995% pure) and N_2 regulated by thermal mass-flow controllers, and fuel by HPLC pump (Shimadzu® LC10 VP).

● *n*-pentane (>99% pure from Sigma-Aldrich®) and O_2 are diluted by N_2 , and injected separately, to avoid oxidation before reaching the injectors .

● Thermal homogeneity is checked using Pt/Pt-Rh10%, 0.1mm diam.

● Oxidation gases are **bubbled in cooled acetonitrile** (0°C, 25 ml, 75 min) after **sonic probe sampling**. Samples are stored in a freezer at -15 °C.

Conditions: **2500 ppm** of ***n*-pentane**, 4 % of O_2 and 95.75 % of N_2
Pressure: **10 atm**
Temperature: **520-800 K**
Equivalence ratio(**ϕ**): **0.5**
Residence time: **1.5 s**

b. Ultra-high pressure liquid chromatography (UHPLC) coupled to high resolution mass spectrometry HRMS (Orbitrap Q-Exactive)

Step 1: Chromatographic separation

C_{18} RP-**UHPLC** (Phenomenex Luna®, 100x2.1 mm, 1.6µm, 100 Å)

Mobile phase: **H_2O+ ACN** (3 to 100% of ACN, flow rate 250 µl/min during 18 min)

b. Ultra-high pressure liquid chromatography (UHPLC) coupled to high resolution mass spectrometry HRMS (Orbitrap Q-Exactive)

Step 1: Chromatographic separation

C_{18} RP-**UHPLC** (Phenomenex Luna®, 100x2.1 mm, 1.6µm, 100 Å)

Mobile phase: **H_2O+ ACN** (3 to 100% of ACN, flow rate 250 µl/min during 18 min)

Step 2: Soft ionization

Atmospheric pressure chemical ionization (**APCI**)
in positive $[M+H]^+$ and negative $[M-H]^-$ modes

b. Ultra-high pressure liquid chromatography (UHPLC) coupled to high resolution mass spectrometry HRMS (Orbitrap Q-Exactive)

Step 1: Chromatographic separation

C_{18} RP-**UHPLC** (Phenomenex Luna®, 100x2.1 mm, 1.6µm, 100 Å)

Mobile phase: **H_2O+ ACN** (3 to 100% of ACN, flow rate 250 µl/min during 18 min)

Step 2: Soft ionization

Atmospheric pressure chemical ionization (**APCI**) in positive $[M+H]^+$ and negative $[M-H]^-$ modes

Step 3: Mass identification

Orbitrap Q-Exactive mass spectrometer

Resolution 140,000
Mass accuracy < 1 ppm

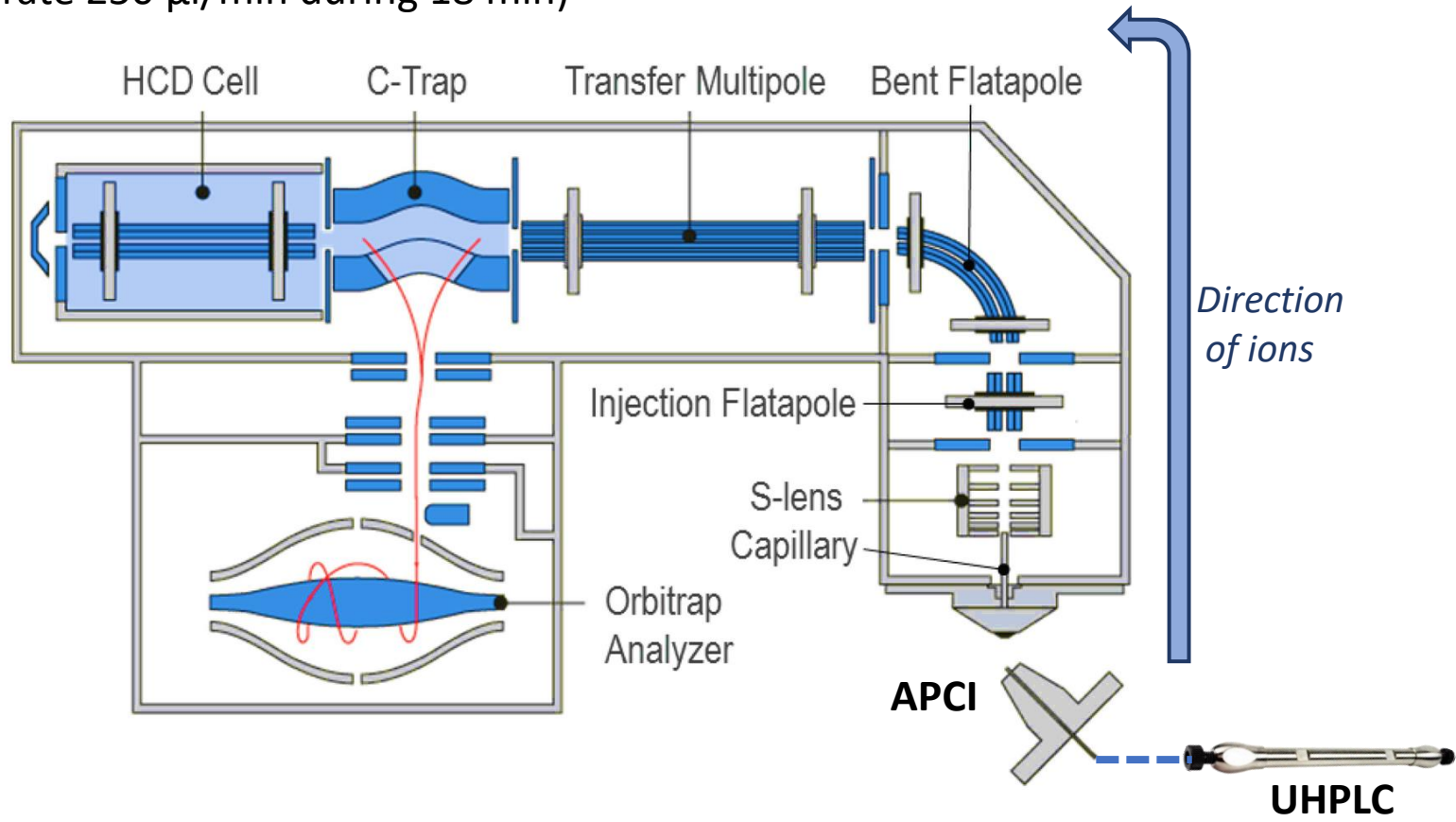

Chemical characterization

OOH function → Isotopic **H/D exchange** (using of D_2O)

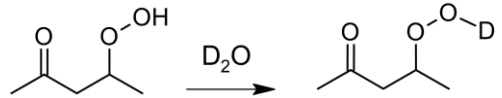

C=O function → **DNPH derivatization** (2,4-dinitrophenylhydrazine)

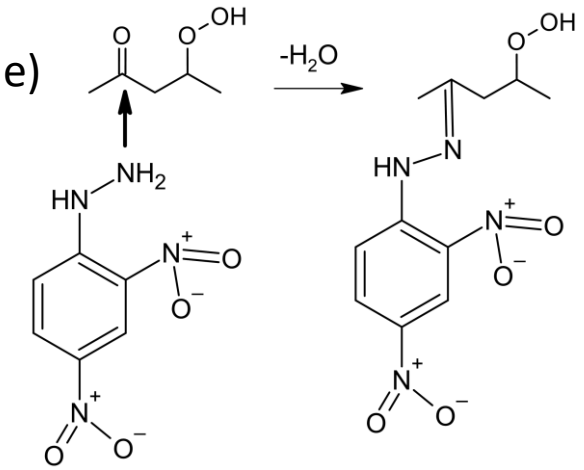

3- Results

3.1. Hydroperoxides

peroxidation of fuel's radicals and H-atom abstraction by $RO_2^{\bullet}$

$$R^{\bullet} + O_2 \rightleftarrows RO_2^{\bullet}$$
$$RO_2^{\bullet} + R'H \rightarrow ROOH + R'^{\bullet}$$
$$RO_2^{\bullet} + HO_2^{\bullet} \rightarrow ROOH + O_2$$

3- Results

3.1. Hydroperoxides

3.1.1. Alkyl-hydroperoxides

peroxidation of fuel's radicals and H-atom abstraction by $RO_2^{\bullet}$

$R^{\bullet} + O_2 \rightleftarrows RO_2^{\bullet}$

$RO_2^{\bullet} + R'H \rightarrow ROOH + R'^{\bullet}$

$RO_2^{\bullet} + HO_2^{\bullet} \rightarrow ROOH + O_2$

Alkyl-hydroperoxides $C_3H_8O_2$, $C_4H_{10}O_2$ and **$C_5H_{12}O_2$**

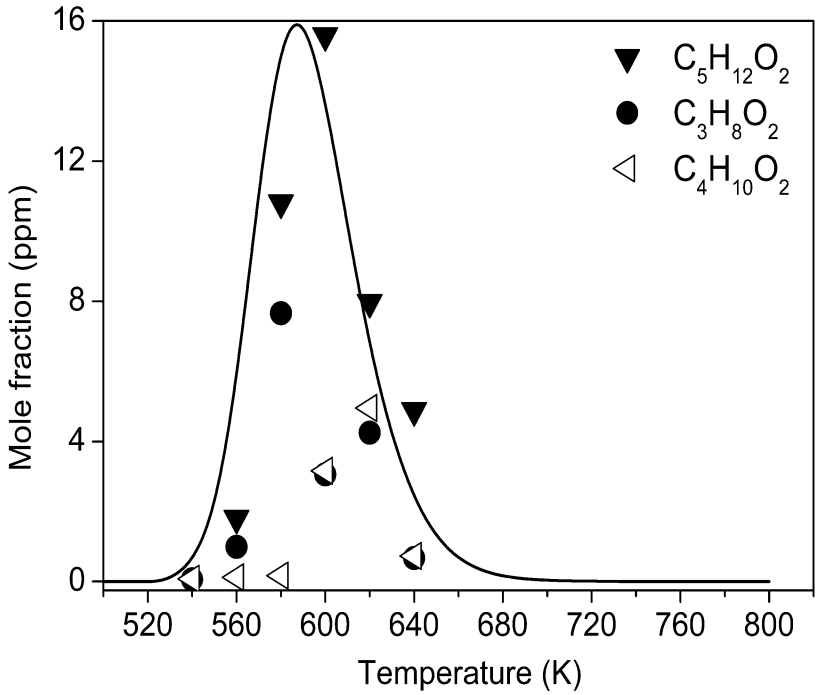

3- Results

3.1. Hydroperoxides

3.1.1. Alkyl-hydroperoxides

peroxidation of fuel's radicals and H-atom abstraction by $RO_2^\bullet$

$R^\bullet + O_2 \rightleftarrows RO_2^\bullet$

$RO_2^\bullet + R'H \rightarrow ROOH + R'^\bullet$

$RO_2^\bullet + HO_2^\bullet \rightarrow ROOH + O_2$

Alkyl-hydroperoxides $C_3H_8O_2$, $C_4H_{10}O_2$ and **$C_5H_{12}O_2$**

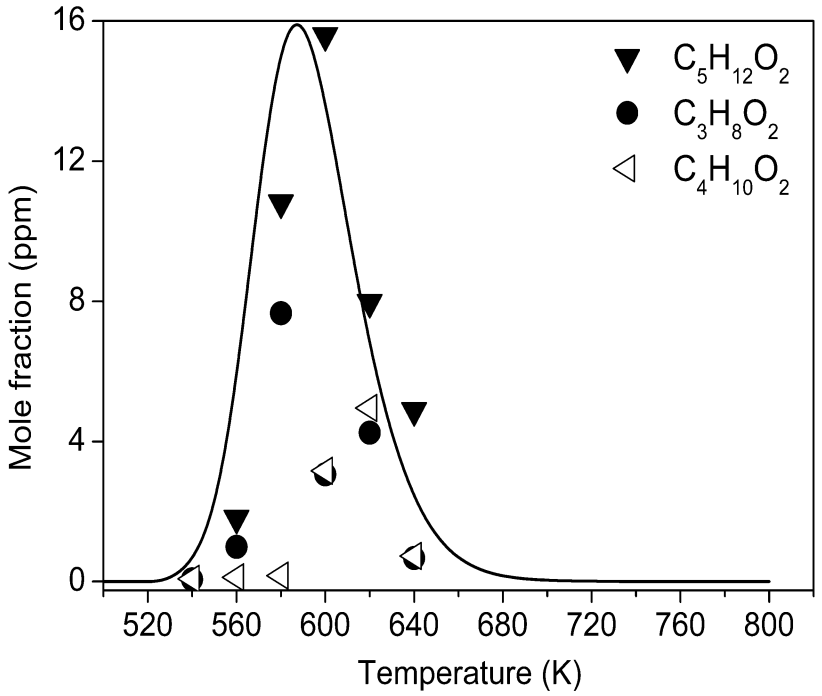

- Are not formed at the same level ($C_5 > C_3 > C_4$)
- Do not peak at the same temperature
  600 K for $C_5H_{12}O_2$, 620 K for $C_4H_{10}O_2$, and 580 K for $C_3H_8O_2$
- A **slight underestimation** of the temperature at which maximum formation of $C_5H_{12}O_2$ occurs (**WS model [30]:** ~585 K vs. 600 K in experiments

No modeling data for C_3 and C_4 alkyl-hydroperoxides

[30] Z. D. Wang; S. M. Sarathy, Third O-2 addition reactions promote the low-temperature auto-ignition of n-alkanes, Combust. Flame 165 (2016) 364-372

3.1.2. Alkenyl-hydroperoxides

Decomposition of $C_5H_{12}O_2$ hydroperoxides → **Alkenylhydroperoxides: $C_2H_4O_2$, $C_3H_6O_2$, $C_4H_8O_2$,** and **$C_5H_{10}O_2$**

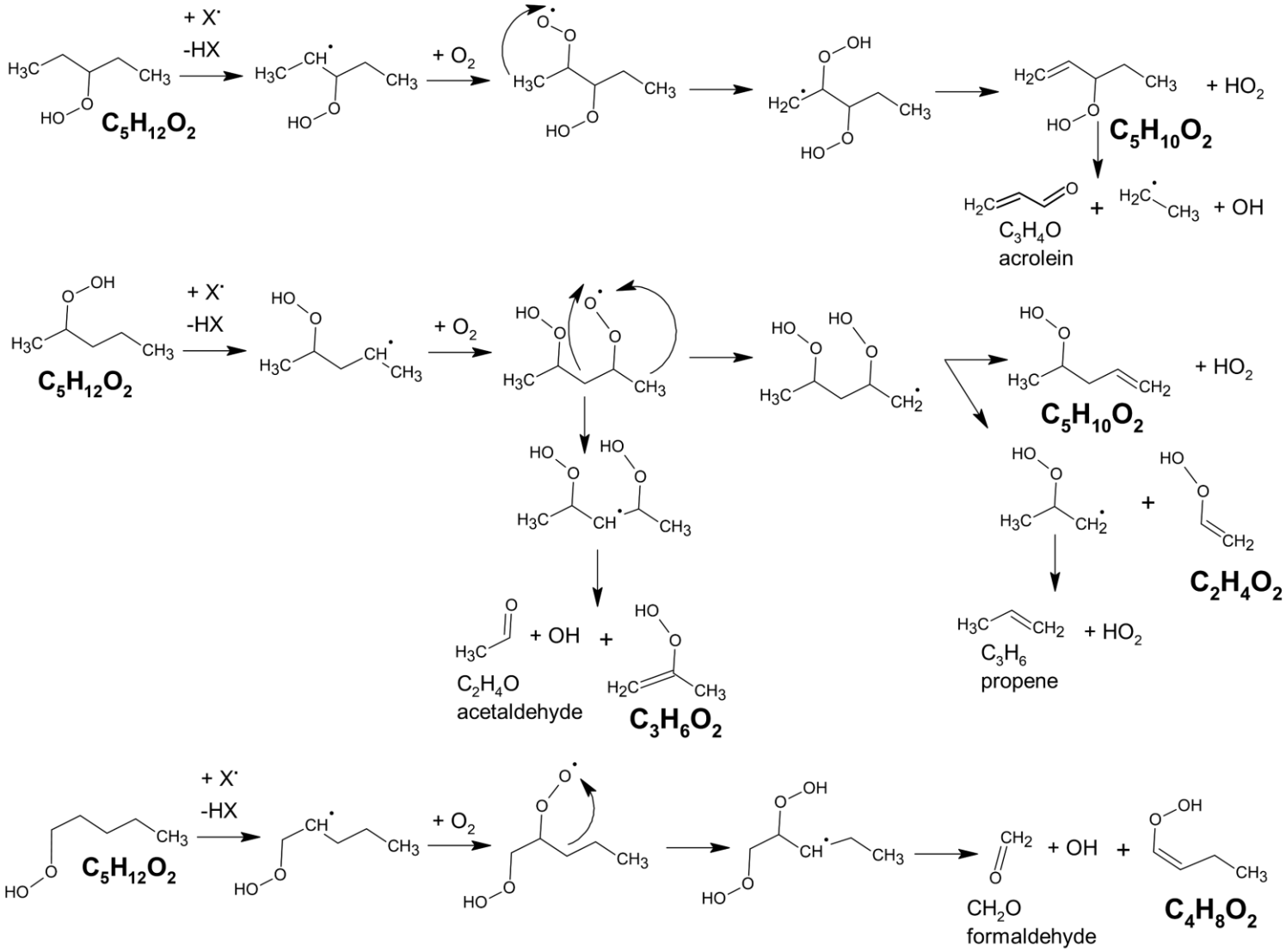

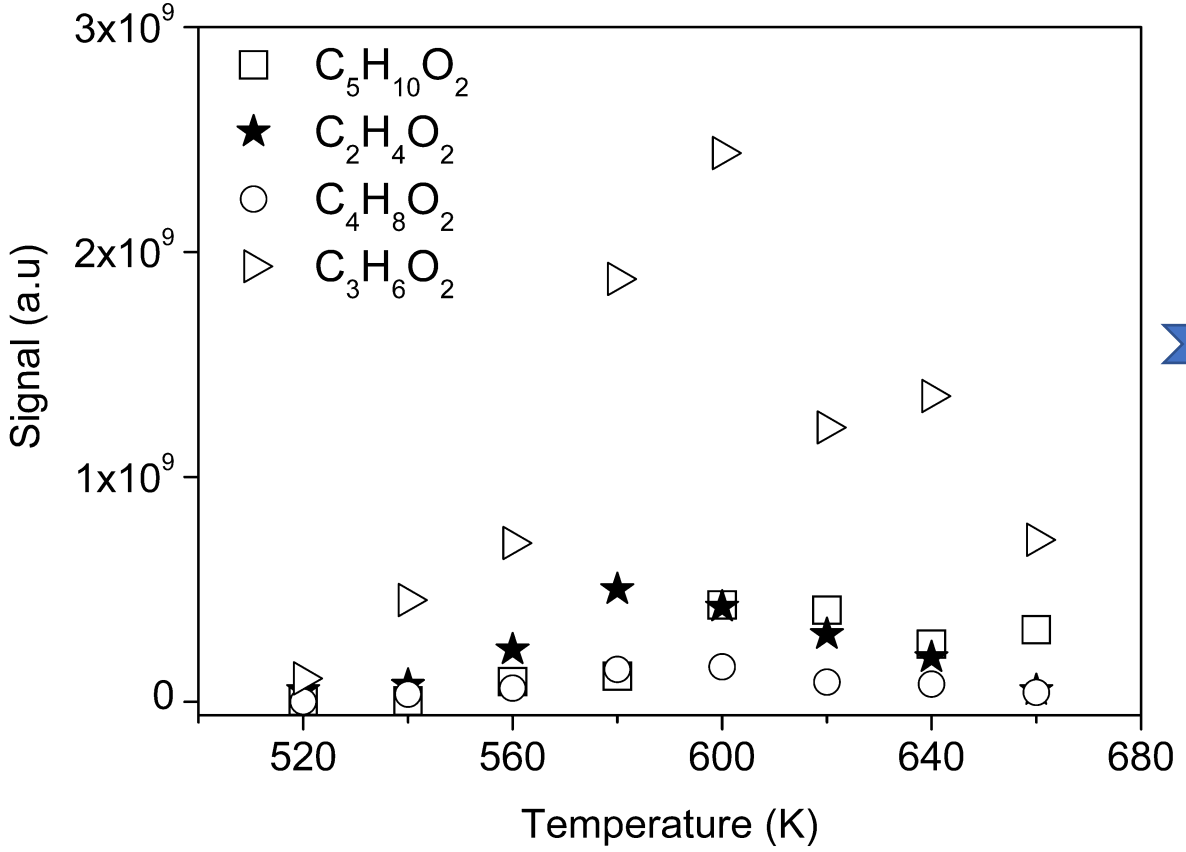

Are not formed at the same level ($C_3>C_2>C_5>C_4$)

Do not peak at the same temperature:
600 K for $C_5H_{10}O_2$, $C_4H_8O_2$ and $C_3H_6O_2$, and 580 K for $C_2H_4O_2$

No modeling results

3.2 Ketohydroperoxides (KHPs)

KHPs are produced from two O_2 additions on fuel's radical: Fuel + $X^{\bullet}$ ($^{\bullet}OH$, $H^{\bullet}$, $O^{\bullet}$, $HO_2^{\bullet}$, O_2 etc.) → $R^{\bullet}$ + XH;
$R^{\bullet} + O_2 \rightarrow RO_2^{\bullet} \rightarrow {}^{\bullet}QOOH$ (H-shift); $^{\bullet}QOOH + O_2 \rightarrow {}^{\bullet}OOQOOH \rightarrow$ **HOOQ'=O** + $^{\bullet}OH$

3.2 Ketohydroperoxides (KHPs)

KHPs are produced from two O_2 additions on fuel's radical: Fuel + $X^{\bullet}$ ($^{\bullet}OH$, $H^{\bullet}$, $O^{\bullet}$, $HO_2^{\bullet}$, O_2 etc.) → $R^{\bullet}$ + XH;
$R^{\bullet} + O_2 \rightarrow RO_2^{\bullet} \rightarrow {}^{\bullet}QOOH$ (H-shift); $^{\bullet}QOOH + O_2 \rightarrow {}^{\bullet}OOQOOH \rightarrow$ **HOOQ'=O** + $^{\bullet}OH$

Signals corresponding to $C_5H_{10}O_3$ KHPs, were detected using UHPLC-HRMS/ APCI +/- ($C_5H_{11}O_3^+$ *m/z* 119.0702) , and negative ($C_5H_9O_3^-$ *m/z* 117.0556)

3.2 Ketohydroperoxides (KHPs)

KHPs are produced from two O_2 additions on fuel's radical: Fuel + $X^{\bullet}$ ($^{\bullet}OH$, $H^{\bullet}$, $O^{\bullet}$, $HO_2^{\bullet}$, O_2 etc.) → $R^{\bullet}$ + XH;
$R^{\bullet} + O_2 \rightarrow RO_2^{\bullet} \rightarrow {}^{\bullet}QOOH$ (H-shift); $^{\bullet}QOOH + O_2 \rightarrow {}^{\bullet}OOQOOH \rightarrow$ **HOOQ'=O** + $^{\bullet}OH$

Signals corresponding to $C_5H_{10}O_3$ KHPs, were detected using UHPLC-HRMS/ APCI +/- ($C_5H_{11}O_3^+$ *m/z* 119.0702) , and negative ($C_5H_9O_3^-$ *m/z* 117.0556)

H/D exchange: *m/z* **120.0761** corresponding to $\mathbf{C_5H_{10}D_1O_3^+}$

DNPH derivatization: *m/z* **297.0840** corresponding to $\mathbf{C_{11}H_{13}O_6N_4^-}$ derivative ($C_5H_{10}O_3$+DNPH)

3.2 Ketohydroperoxides (KHPs)

KHPs are produced from two O_2 additions on fuel's radical: Fuel + $X^{\bullet}$ ($^{\bullet}OH$, $H^{\bullet}$, $O^{\bullet}$, $HO_2^{\bullet}$, O_2 etc.) → $R^{\bullet}$ + XH;
$R^{\bullet} + O_2 \rightarrow RO_2^{\bullet} \rightarrow {}^{\bullet}QOOH$ (H-shift); $^{\bullet}QOOH + O_2 \rightarrow {}^{\bullet}OOQOOH \rightarrow$ **HOOQ'=O** + $^{\bullet}OH$

Signals corresponding to $C_5H_{10}O_3$ KHPs, were detected using UHPLC-HRMS/ APCI +/- ($C_5H_{11}O_3^+$ *m/z* 119.0702) , and negative ($C_5H_9O_3^-$ *m/z* 117.0556)

H/D exchange: *m/z* **120.0761** corresponding to $\mathbf{C_5H_{10}D_1O_3^+}$

DNPH derivatization: *m/z* **297.0840** corresponding to $\mathbf{C_{11}H_{13}O_6N_4^-}$ derivative ($C_5H_{10}O_3$+DNPH)

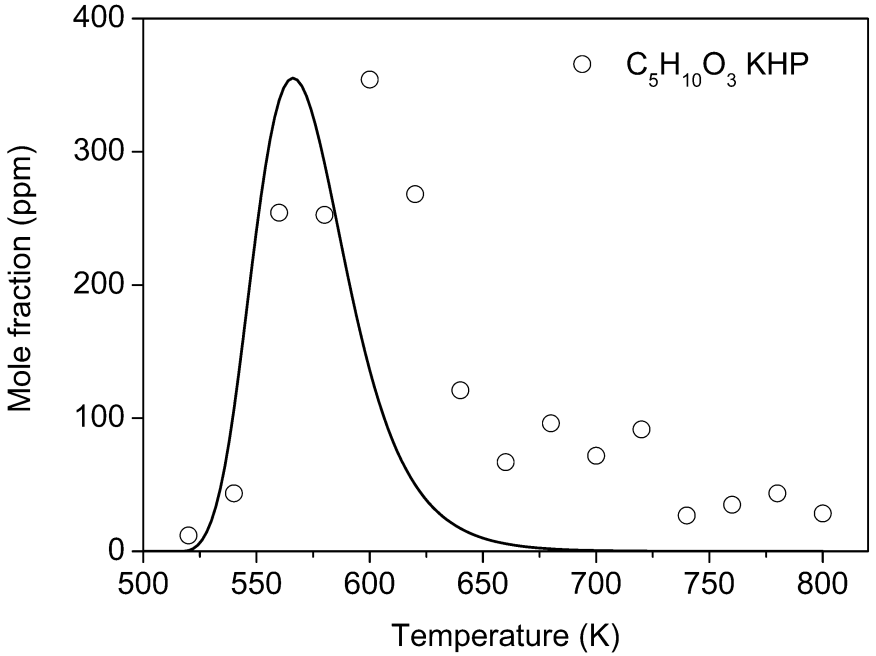

Underestimation of the temperature at which maximum formation of $C_5H_{10}O_3$ is observed (**WS model [30]:** ~580 K vs. measurements: 600 K)

[30] Z. D. Wang; S. M. Sarathy, Third O-2 addition reactions promote the low-temperature auto-ignition of n-alkanes, Combust. Flame 165 (2016) 364-372

Decomposition of $C_5H_{10}O_3$ hydroperoxides

Lower mass KHPs: $C_4H_8O_3$, and **$C_3H_6O_3$**

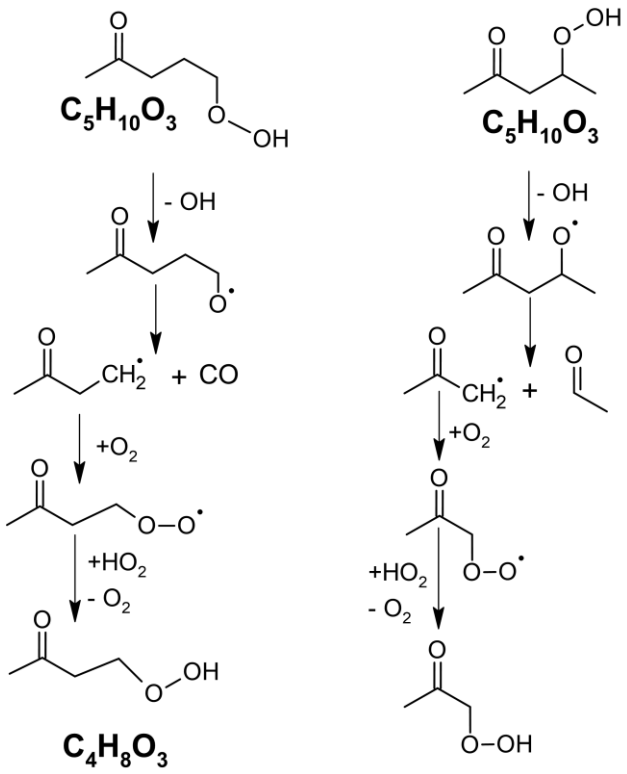

Decomposition of $C_5H_{10}O_3$ hydroperoxides

Lower mass KHPs: $C_4H_8O_3$, and **$C_3H_6O_3$**

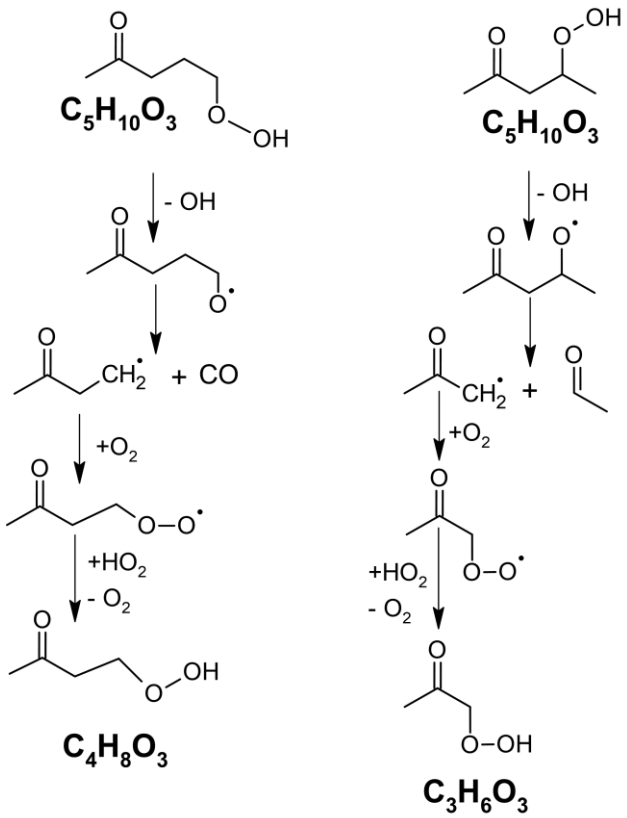

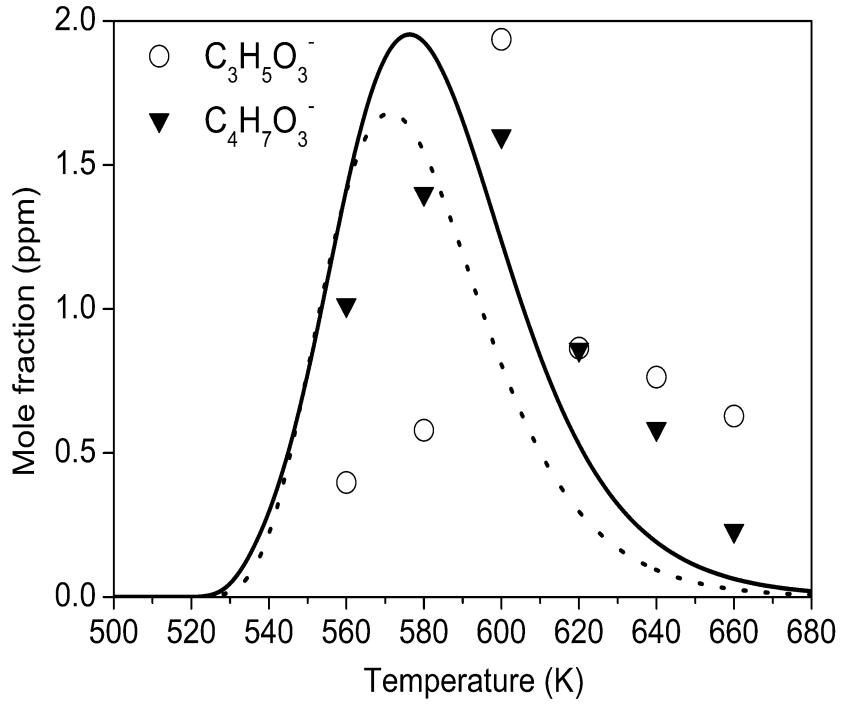

Underestimation of the temperature at which maximum formation of $C_3H_6O_3$ and $C_4H_8O_3$ occurs (**WS model [30]:** ~580 and 575 K, respectively, vs. 600K in experiments.

[**30]** Z. D. Wang; S. M. Sarathy, Third O-2 addition reactions promote the low-temperature auto-ignition of n-alkanes, Combust. Flame 165 (2016) 364-372

3.3 Highly oxygenated molecules (HOMs)

Highly oxygenated molecules result from the addition of multiple molecules of O_2 on *n*-pentyl radicals.

Dihydroperoxides (**$C_5H_{12}O_4$**), **olefinic dihydroperoxides** (**$C_5H_{10}O_4$**), and **diketo-hydroperoxides** (**$C_5H_8O_4$**) were detected using negative APCI HRMS ($C_5H_{11}O_4^-$, *m/z* 135.0663, $C_5H_9O_4^-$, *m/z* 133.0506, $C_5H_7O_4^-$, *m/z* 131.0350).

3.3 Highly oxygenated molecules (HOMs)

Highly oxygenated molecules result from the addition of multiply molecules of O_2 on *n*-pentyl radicals.

Dihydroperoxides (**$C_5H_{12}O_4$**), **olefinic dihydroperoxides** (**$C_5H_{10}O_4$**), and **diketo-hydroperoxides** (**$C_5H_8O_4$**) were detected using negative APCI HRMS ($C_5H_{11}O_4^-$, *m/z* 135.0663, $C_5H_9O_4^-$, *m/z* 133.0506, $C_5H_7O_4^-$, *m/z* 131.0350).

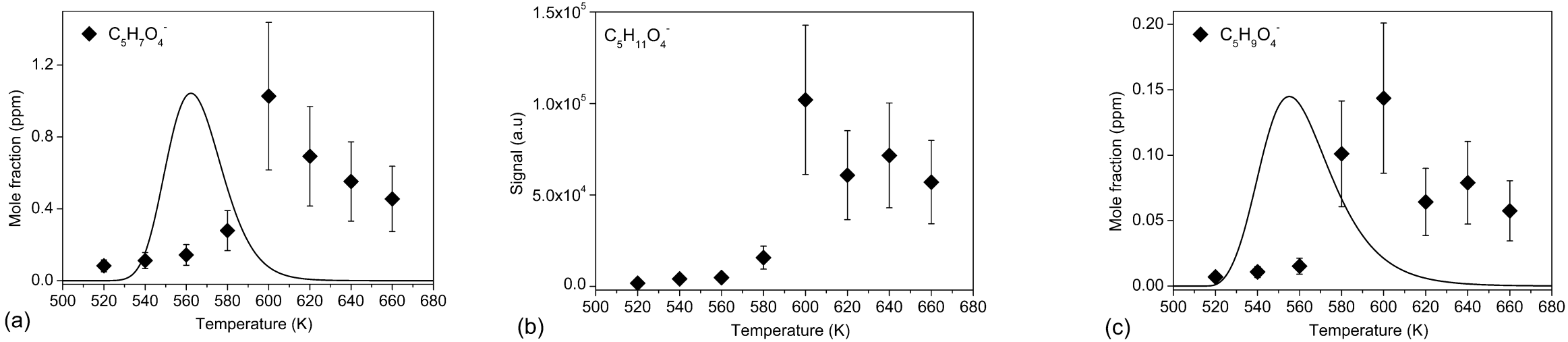

Underestimation of the temperature at which the maximum formation of $C_5H_8O_4$ and $C_5H_{10}O_4$ is observed (**WS model [30] :** ~555 K and 560 K, respectively, vs. 600 K in experiments)

[30] Z. D. Wang; S. M. Sarathy, Third O-2 addition reactions promote the low-temperature auto-ignition of n-alkanes, Combust. Flame 165 (2016) 364-372

No modeling data for $C_5H_{12}O_4$

4- Conclusion and perspectives

This work highlighted the presence of *n*-pentane low-temperature oxidation intermediates never or rarely reported before (**C_3-C_5 alkyl-hydroperoxides, C_2-C_5 alkenyl-hydroperoxides**, **C_3-C_5 keto-hydroperoxides**, and **HOMs ($C_5H_8O_4$, $C_5H_{12}O_4$, $C_5H_{10}O_4$)**.

Other oxidation products (2-Me-THF, 2- and 3-pentanone, 2,4-pentanedione, 3-penten-2-one, 2-butanone, 2,5-DHF, MVK etc.) were detected using UHPLC-HRMS analyses

Further investigations of *n*-pentane oxidation using other laboratory experiments, e.g., **piston engines** or **rapid compression machines** (**RCM**)

Acknowledgements

The authors gratefully acknowledge funding from the Labex Caprysses (convention ANR-11-LABX-0006-01) and from the Région Centre Val de Loire, EFRD, and CPER (projects PROMESTOCK and APROPOR-E).